Morphological, electrical, and optical properties of InN grown by hydride vapor phase epitaxy on sapphire and template substrates

D. Y. Song, V. Kuryatkov, M. Basavaraj, D. Rosenbladt, S. A. Nikishin,[a] and M. Holtz
Texas Tech University, Lubbock, Texas 79409

A. L. Syrkin, A. S. Usikov, V. A. Ivantsov, and V. A. Dmitriev
TDI, Inc., 12214 Plum Orchard Drive, Silver Spring, Maryland 20904

(Received 2 November 2005; accepted 7 April 2006; published online 6 June 2006)

We report studies of the morphological, electrical, and optical properties of InN grown by hydride vapor phase epitaxy. The layers have been grown on *c*-plane sapphire substrates and epitaxial GaN, $Al_{0.7}Ga_{0.3}N$, and AlN templates grown on sapphire. InN properties are found to depend on template type with improvement of crystal structure in the template substrate order AlN→AlGaN→GaN. X-ray studies reveal InN layers grown on template substrates to be relaxed with lattice constants $a=3.542$ Å and $c=5.716$ Å. The Raman spectra and optical gaps of the InN layers, vary with free-carrier concentration in agreement with previous studies. We obtain a value of 2.5 ± 0.2 for the index of refraction of InN. © *2006 American Institute of Physics*. [DOI: 10.1063/1.2201856]

Recently, there has been considerable interest in InN as a prospective narrow band gap semiconductor[1] with an intrinsic energy gap to be ~0.7 eV.[2–4] The energy gap of InN has been the subject of controversy. Recent work has interpreted the range of values based on free-carrier concentration and band filling;[5] alternative explanations rely on deviations in the In composition as a result of cluster formation.[6]

The growth of high-quality InN remains challenging. One general difficulty in growing III-nitrides is the necessity to use foreign substrates which the lattice constant are not well suited to epitaxy. The mismatch between InN and sapphire is even worse than for either AlN or GaN.

We report the physical properties of InN grown by hydride vapor phase epitaxy (HVPE) on sapphire and on epitaxial layers of GaN, AlN, and $Al_{0.7}Ga_{0.3}N$, each grown on sapphire substrates. HVPE has been demonstrated for growing materials with low defect concentrations and with rapid deposition rates.[7–9] However, there are few papers exploring HVPE as a growth method for InN.[10–12]

The growth processes are carried out at atmospheric pressure in a hot-wall quartz tube reactor with a resistively heated furnace. Commercial 2 in. (0001) *c*-plane sapphire, along with GaN, AlN, and $Al_{0.7}Ga_{0.3}N$ layers grown by HVPE on identical sapphire wafers, is used as substrates. Properties of the templates have been described elsewhere.[13,14] The template epilayers are around 1 μm thick and InN layers are ~200 nm thick. Growth temperature of the InN is varied from 500 to 600 °C. Deposition time varies from 20 to 30 min.

We study surface morphology by scanning electron microscope (SEM) and crystal structure by x-ray diffraction (XRD). For continuous InN layers we have also studied the room-temperature properties by Hall measurements and optical spectroscopy. Micro-Raman spectra were measured using the argon ion 488.0 nm laser line as excitation. Optical reflectance and transmittance measurements were carried out across the wavelength range of 200–900 nm.

Hall measurements show all samples to be heavily conducting with resistivity of $\sim10^{-4}$ Ω cm. The electron concentrations range from $\sim10^{20}$ to $\sim10^{21}$ cm^{-3} with corresponding mobilities from 105 to 12 cm^2/V s. The high electron concentration is due to a combination of intentional and unintentional dopings.

In Fig. 1 we show SEM images illustrating the two extreme cases of InN morphology. Figure 1(a) shows InN grown directly on sapphire and having the microcolumnar

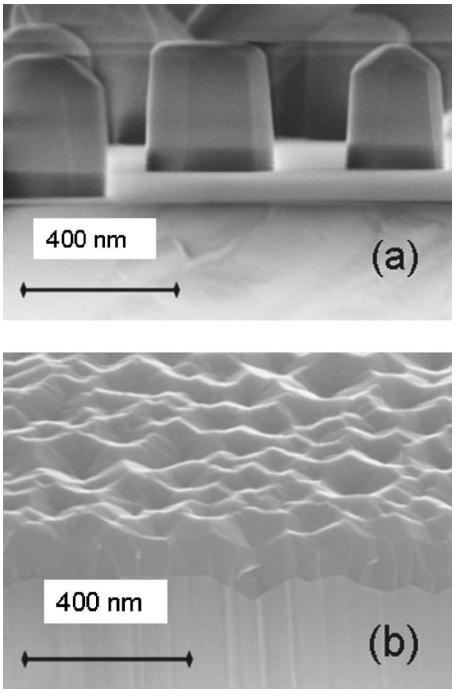

FIG. 1. SEM images of InN grown directly on the sapphire substrate (a) and on the GaN template (b).

[a]Author to whom correspondence should addressed; electronic mail: sergey.a.nikishin@ttu.edu

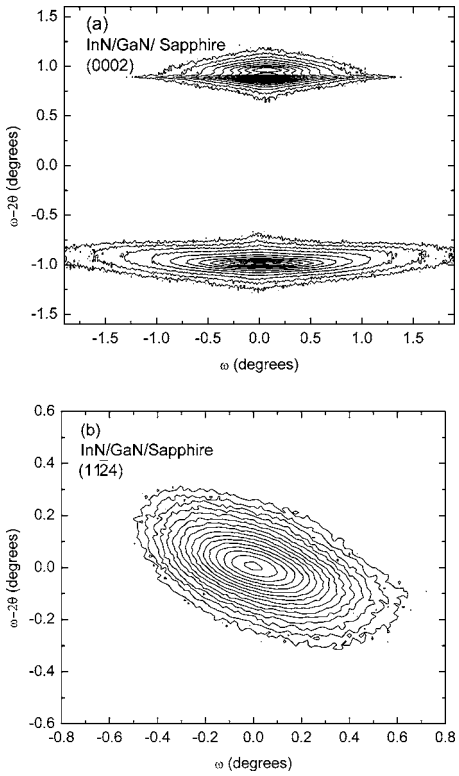

FIG. 2. X-ray RSM of InN grown on GaN template: (a) is for (0002) and (b) is for (11$\bar{2}$4).

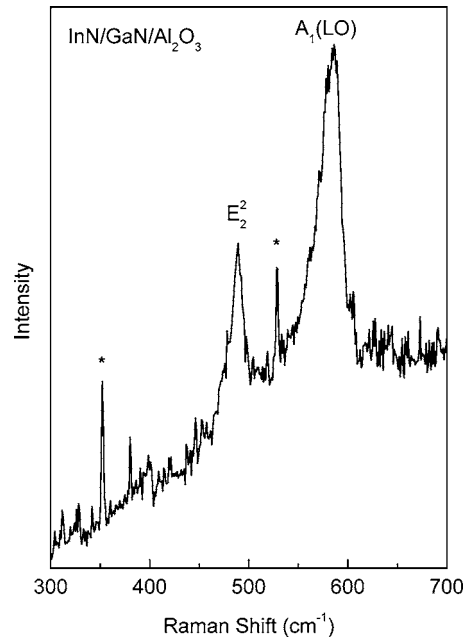

FIG. 3. Raman spectrum of InN grown on GaN template. The asterisk indicates argon ion laser plasma lines.

structure. The diameters and heights of these columns vary from 200 to 350 nm and from 500 nm to several microns, respectively. Typical lateral and vertical growth rates for these InN columns are ~15 and ~18.5 nm/min, respectively. XRD measurements in ω scanning geometry show the full width at half maximum (FWHM) of the (0002) peak to be ~110 arc sec, indicating very good crystalline quality of InN columnar material.

The SEM image in Fig. 1(b) shows the InN grown on the GaN epitaxial layer. Clearly seen is layer surface morphology following that of the substrate. From XRD measurements the lattice constants of the InN grown on GaN are a =3.542 Å and c=5.716 Å.[15] For InN grown on the AlN and AlGaN templates, lattice constants agree with these same values with standard deviations of 0.002 and 0.006 Å for a and c, respectively. The InN layers grown on GaN exhibited the smoothest surface morphology.

For InN layers grown on GaN templates, the FWHM for x-ray rocking curves measured using ω-scanning geometry is about 400 and 1600 arc sec for the (10$\bar{1}$2) and (0002) reflections, respectively. Figure 2(a) shows the x-ray reciprocal space map (RSM) of the InN epilayer along the symmetrical (0002) axis. Well-defined Bragg peaks indicate the single crystalline nature of the sample. The two peaks are aligned along ω=0, confirming that the InN layer grows in plane with the underlying GaN layer. The broadening in the ω direction indicates an angular spread of the mosaic blocks. The RSM results indicate inhomogeneous strain which we attribute to the InN/GaN interface region. For the same sample we measured the RSM close to the (11$\bar{2}$4) reflection with grazing angle of incidence of the x-ray beam in rocking curve mode, Fig. 2(b). The elliptical nature is consistent with the mosaic morphology of the InN. The mosaic block sizes and tilt produce diffuse scattering.[16,17] For this sample, we obtain a lateral correlation length of 106 nm and a microscopic tilt of 0.17°. We note that the InN layers grown on AlGaN and AlN templates have similar XRD line shapes, but the FWHM increases in the order GaN → AlGaN → AlN. We tentatively attribute this rising trend to increasing lattice constant mismatch between the InN and epitaxial template and to the presence of native aluminum oxide islands.[18]

The Raman spectrum for the InN/GaN sample is given in Fig. 3. Spectra from the other samples grown on AlN and AlGaN templates were consistent with the one shown. Two features are observed at 489 and 584 cm^{-1} corresponding to the E_2^2 and A_1(LO) symmetry-allowed zone-center phonons in backscattering along [0001]. Previous measurements of epitaxial InN identify the E_2^2 phonon ranging from 488 to 490 cm^{-1} in energy,[19,20] with one report of 495 cm^{-1}.[21] The E_2^2 phonon is commonly used in GaN and AlN to determine stress induced by the substrate.[22,23]. The InN phonon energies were all within ±1 cm^{-1} indicating that all layers studied are relaxed in agreement with the XRD results.

The Raman feature at 584 cm^{-1} is related to the A_1(LO) phonon. The bare LO phonons are not expected in heavily doped material due to the plasmon-phonon interaction. Rather, two phonon-plasmon coupled modes are expected above and below the LO and TO vibrational energies, respectively. In GaN, heavy doping completely quenches the intensity of the A_1(LO) feature.[24] In our measurements on InN, we observe neither a shift nor a decreased intensity with higher values of carrier concentration. The presence of relatively intense A_1(LO) scattering in heavily doped InN have recently been attributed to a charge density fluctuation scattering mechanism at finite wave vector.[20]

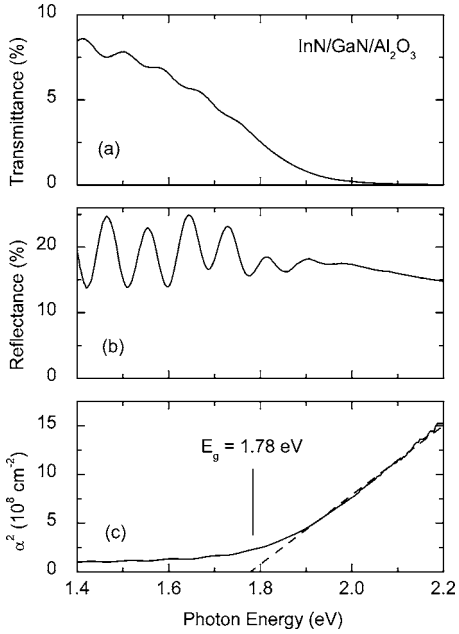

FIG. 4. Transmittance (a) and reflectance (b) spectra of InN grown on GaN template. Square of the absorption coefficient is shown in (c) obtained from reflectance and transmission measurements.

Figure 4 presents optical measurements of the InN layer grown on epitaxial GaN. Panel (a) shows transmittance (T) at normal incidence and panel (b) exhibits the reflectance (R) at 5° external angle of incidence. The transmission is high below photon energy ~1.8 eV, above which it decreases as the InN becomes opaque. The reflectance exhibits Fabry-Pérot fringes in the transparent range. The energy at which these fringes are quenched by the onset of high absorption is a measure of the optical energy gap.[25] Using the method presented by Poruba *et al.*,[26] the spectra are used to obtain the absorption coefficient (α) and index of refraction. For transitions across direct band gap semiconductors, the absorption depends on photon energy according to

$$\alpha(\hbar\omega) \propto \sqrt{\hbar\omega - E_g}, \tag{1}$$

above the optical gap E_g. In Fig. 4(c) we graph α^2 versus photon energy. Extrapolating the linear fit of α^2 versus photon energy data to $\alpha^2=0$ provides an estimate for E_g. For the InN/GaN structure illustrated, we obtain optical gap of $E_g = 1.78 \pm 0.05$ eV. The magnitude of α is in agreement with previous work on InN.[27]

The reflectance and transmittance analysis was also carried out for all InN samples grown on AlN and AlGaN templates. We obtain optical energy gaps in the range of 1.44–1.78 eV, for samples with carrier concentrations of $\sim 10^{20}$ and $\sim 10^{21}$ cm^{-3}, respectively. Variations in the optical gap of InN have been attributed to band filling through the Burstein-Moss effect.[5] We have examined the effect of band filling on the optical gap of InN using Kane's two-band model with nonparabolic conduction band dependence and adopting the value of 0.7 eV for the band gap of undoped InN.[3] We find basic agreement with the trend of our data. However, improvements in the agreement are obtained by taking into account conduction band renormalization effects from electron-electron correlation and electron-ionized impurity interactions.[28] Our optical analysis results in a value of the index of refraction for InN of 2.5 ± 0.2 for photon energies below the optical energy gap and independent of carrier concentration over the range $\sim 10^{20}$–10^{21} cm^{-3}.

In conclusion, we have examined InN grown by HVPE on sapphire and epitaxial GaN, AlGaN, and AlN templates. Under identical growth conditions, the InN morphology is found to vary from columnar, when grown on sapphire, to continuous layers, when grown on the epitaxial templates. The electron concentrations measured by Hall method range from $\sim 10^{20}$ to $\sim 10^{21}$ cm^{-3} with corresponding mobilities from 105 to 12 cm^2/V s. The optical gap is found to be in the 1.4–1.8 eV range and vary with free-carrier concentration.

Work at TTU was supported by the National Science Foundation (ECS-0323640, ECS-0304224) and the J. F. Maddox Foundation. Work at TDI, Inc. was partly supported by the U.S. Department of Energy (DE-FG02-03ER83802).

[1] A. G. Bhuiyan, A. Hashimoto, and A. Yamamoto, J. Appl. Phys. **94**, 2779 (2003).
[2] V. Y. Davydov *et al.*, Phys. Status Solidi B **229**, R1 (2002).
[3] J. Wu *et al.*, Appl. Phys. Lett. **80**, 3967 (2002).
[4] T. Matsuoka, H. Okamoto, M. Nakao, H. Harima, and E. Kurimoto, Appl. Phys. Lett. **81**, 1246 (2002).
[5] J. Wu, W. Walukiewicz, W. Shan, K. M. Yu, J. W. Ager, E. E. Haller, H. Lu, and W. J. Schaff, Phys. Rev. B **66**, 201403 (2002).
[6] T. V. Shubina *et al.*, Phys. Rev. Lett. **92**, 117407 (2004).
[7] H. P. Maruska and J. J. Tietjen, Appl. Phys. Lett. **15**, 327 (1969).
[8] M. W. Yim, E. J. Stofko, P. J. Zauaucchi, J. I. Pankove, M. Ettenburg, and S. L. Gilbert, J. Appl. Phys. **44**, 292 (1973).
[9] J. Hagen, R. D. Metcalfe, D. Wickenden, and W. Clark, J. Phys. C **11**, L143 (1978).
[10] L. A. Marasina, I. G. Pichugin, and M. Tlaczala, Krist. Tech. **12**, 541 (1977).
[11] Y. Sato and S. Sato, J. Cryst. Growth **144**, 15 (1994).
[12] N. Takahashi, R. Matsumoto, A. Koukitu, and H. Seki, Jpn. J. Appl. Phys., Part 2 **36**, L743 (1997).
[13] A. S. Usikov *et al.*, Phys. Status Solidi C **7**, 2580 (2003).
[14] D. Tsvetkov, Y. Melnik, A. Davydov, A. Shapiro, O. Kovalenkov, J. B. Lam, and J. J. Song, Phys. Status Solidi A **188**, 429 (2001).
[15] O. K. Semchinova, J. Aderhold, J. Graul, A. Filimonov, and H. Neff, Appl. Phys. Lett. **83**, 5440 (2003).
[16] P. F. Fewster, V. Holy, and N. L. Andrew, Mater. Sci. Semicond. Process. **4**, 475 (2001).
[17] R. Chierchia, T. Bottcher, H. Heinke, S. Einfeldt, S. Figge, and D. Hommel, J. Appl. Phys. **93**, 8918 (2003).
[18] B. Borisov, V. Kuryatkov, Yu. Kudryavtsev, R. Asomoza, S. A. Nikishin, D. Y. Song, M. Holtz, and H. Temkin, Appl. Phys. Lett. **87**, 132106 (2005).
[19] V. Y. Davydov *et al.*, Appl. Phys. Lett. **75**, 3297 (1999).
[20] F. Demangeot, C. Pinquier, J. Frandon, M. Gaio, O. Briot, B. Maleyre, S. Ruffenach, and B. Gil, Phys. Rev. B **71**, 104305 (2005).
[21] H. J. Kwon, Y. H. Lee, O. Miki, H. Yamano, and A. Yoshida, Appl. Phys. Lett. **69**, 937 (1996).
[22] M. Holtz, M. Seon, T. Prokofyeva, H. Temkin, R. Singh, F. P. Dabkowski, and T. D. Moustakas, Appl. Phys. Lett. **75**, 1757 (1999).
[23] T. Prokofyeva, M. Seon, J. Vanbuskirk, M. Holtz, S. A. Nikishin, N. N. Faleev, H. Temkin, and S. Zollner, Phys. Rev. B **63**, 125313 (2001).
[24] A. S. Zubrilov, S. A. Nikishin, G. D. Kipshidze, V. V. Kuryatkov, H. Temkin, T. I. Prokofyeva, and M. Holtz, J. Appl. Phys. **91**, 1209 (2002).
[25] M. Holtz *et al.*, J. Appl. Phys. **89**, 7977 (2001).
[26] A. Poruba *et al.* J. Appl. Phys. **88**, 148 (2000).
[27] Q. X. Guo, T. Tanaka, M. Nishio, H. Ogawa, X. D. Pu, and W. Z. Shen, Appl. Phys. Lett. **86**, 231913 (2005).
[28] J. Wu *et al.*, Appl. Phys. Lett. **84**, 2805 (2004).